DAMAGE MECHANISMS IN THIN-PLY COMPOSITES : FREE EDGE/BULK MEASUREMENTS AND MULTISCALE MODELLING

Sébastien Kohler[1], Joël Cugnoni[1], Robin Amacher[1], John Botsis[1]

[1]Faculté des sciences et techniques de l'ingénieur, Ecole Polytechnique Fédérale de Lausanne (EPFL),
Bâtiment ME, Station 9, CH-1015 Lausanne, Switzerland
Email : joel.cugnoni@epfl.ch, Web Page : http ://lmaf.epfl.ch

Keywords: Thin-Ply, Acoustic Emission, Damage Mechanisms, Multiscale Modelling, SEM

Abstract
When reducing the ply thickness of polymer matrix fibre reinforced composites, a definite increase in the tensile stress-bearing capability of the transverse constrained plies has been shown to occur. However, the reason for this change in mechanical properties is not yet fully understood. In this work, the damage progression within M40JB/TP80EP unnotched quasi-isotropic symmetric laminate samples ($[45/90/-45/0]_{ns}$) loaded in tension is monitored through simultaneous acoustic emission measurements and optical observation at the edge of the specimens. This experimental data is then compared to a plane-strain multiscale FE model using embedded cells built upon actual observed microstructures.

1. Introduction

High performance carbon fibre reinforced polymer (CFRP) composites have been widely adopted in recent years due to an increasing demand for weight reduction and energy saving. Despite their numerous advantages, CFRP are limited by their intrinsically weak transverse and interlaminar properties which reduces their strength to a fraction (about 30-50%) of the theoretical strength of the fibres. As demonstrated in recent studies [1, 2], thin-ply composites have the potential to delay or even suppress early matrix dominated damages up to the point of fibre failure, and consequently to extend significantly the range of admissible load with respect to current generation of CFRP. However, in the present state of knowledge, several questions remain unanswered, which prevents the wide adoption of this new generation of composite materials.

In the present study, experimental data representing damage events in the bulk of the samples, acquired via acoustic emission measurements, is compared to damage events at the free edge of the same samples, recorded via in-situ microscope observations. Initial results of a multiscale plane-strain FE model are then compared to the bulk measurements.

2. Materials and Methods

2.1. Experimental Study

In order to assess the macro scale damage sequence in thin-ply carbon composite, M40JB/TP80EP unnotched tensile test specimens have been produced in quasi-isotropic ($[45/90/-45/0]_{ns}$) stacking sequences. These samples were produced in the four different ply thicknesses t considered in Amacher et al. [1], namely t = 30 μm, 75 μm, 150 μm and 300 μm using the same Thin Ply Technology prepreg

Excerpt from ISBN 978-3-00-053387-7

material, produced from the same fibre and resin production batches on the same production line in order to minimize potential scatter. All samples had the same dimensions, the thickness of the constituting plies being the only difference between them. The plates were cured in an autoclave following the manufacturer's recommended cycle (peak of 80° C for 8 hours at 3 bar after an initial 2 hour long plateau at 60° C) using a machined aluminium mould to ensure a uniform and constant volume fraction. The volume fraction of all the plates produced was measured between 51,7% and 57,9% with a mean value of 55,5% and a standard deviation of 2,68%. The strength measurements reported here were consequently all normalized to 55% volume fraction to account for this small discrepancy according to the formula $\sigma_{55\%} = \frac{55\%}{vf_n}\sigma_n$, where $\sigma_{55\%}$ is the strength normalized for 55% volume fraction, vf_n the effective volume fraction of each plate and σ_n the strength actually measured during the experiment.

The samples were tested in tension accordingly to the ASTM D3039 standard [3] whilst recording the damage activity by simultaneously performing acoustic emission measurements, and monitoring the visible crack growth on a polished lateral free edge using a video microscope. Similarly, as validated in Amacher et al. [1], the onset of damage was defined as the stress at which the cumulative acoustic energy reaches a 10^{-15}J threshold, as acquired by a Mistras-2001 measurement equipment using a 65dB minimum acquisition threshold and an appropriate ΔT-front-end filter to reject acoustic activity taking place out of the gauge length. This procedure ensures that the reported values were comparable with prior measurements.

Regarding the free edge observations, the faces were polished up to $3\mu m$ grit sanding paper in a fixture ensuring a correct planarity during the polishing. The acquisition speed of the video equipment forced the use of a slower loading speed of 0.125 mm/min to ensure a good resolution of the pictures. The length of the observation window ranges from 3.12mm to 0.8mm in the center of the gauge region, depending on the ply thickness. Lastly, SEM observations at the free edge of selected specimens were performed after testing to ensure that the limited resolution of the optical equipment did not prevent the observation of some defects during the tests.

2.2. Numerical Study

In order to eventually elucidate the effects of constituents on the analysis of damage mechanisms, a FE model was built using a multi-scale "embedded cell" modelling approach in which a finely discretized "micro-mechanics" region corresponding to the 90° ply is embedded in a larger continuum model of the laminate. To account for potential differences (observed qualitatively in microscopy) between microstructures of plies of different thicknesses, microstructures taken from actual sample observations were used to construct the micromechanical zones of the embedded cell. This approach has been shown to work well in the past, as demonstrated for instance in the work of Canal et al. [4]. A transition zone with increasing matrix and interface properties was built-in at the edges of the embedded cell to avoid localization, and the simulation results were only evaluated outside of these zones.

As seen in figure 1, three different microstructures were embedded in a $[0/45/90/-45/0]$ stack to replicate the stress state in a quasi-isotropic sample. A 3D model representing a thin slice of material was used to take advantage of the cohesive surface formulation to model the fibre/matrix interface, and the plane-strain condition were implemented by setting the appropriate boundary conditions on the front and back face of the model, namely a symmetry on one and a planarity constraint on all the nodes of the other one (to allow unconstrained Poisson effects). The fibres were modelled using a linear elastic isotropic model relying on the properties published by the fibre manufacturer. The matrix was modelled using a Drucker-Prager model with regularized damage based on properties measured on bulk matrix specimens and estimated parameters from literature. A linear softening, energy based, cohesive model was used to simulate the damage processes at the fibre-matrix interface using properties estimated from literature and

Excerpt from ISBN 978-3-00-053387-7

experiments performed. Because of the inherent instabilities, the problem was solved using a dynamic explicit solver (Abaqus Explicit) with mass scaling to represent the quasi-static response of the material.

In this study, the point at which the first cracks appear in the micro-modelled region was the key output, with the cracks being defined as the unloading of a zone spanning over at least 4 fibres. This data was then compared to the onset of damage value recorded by acoustic emission.

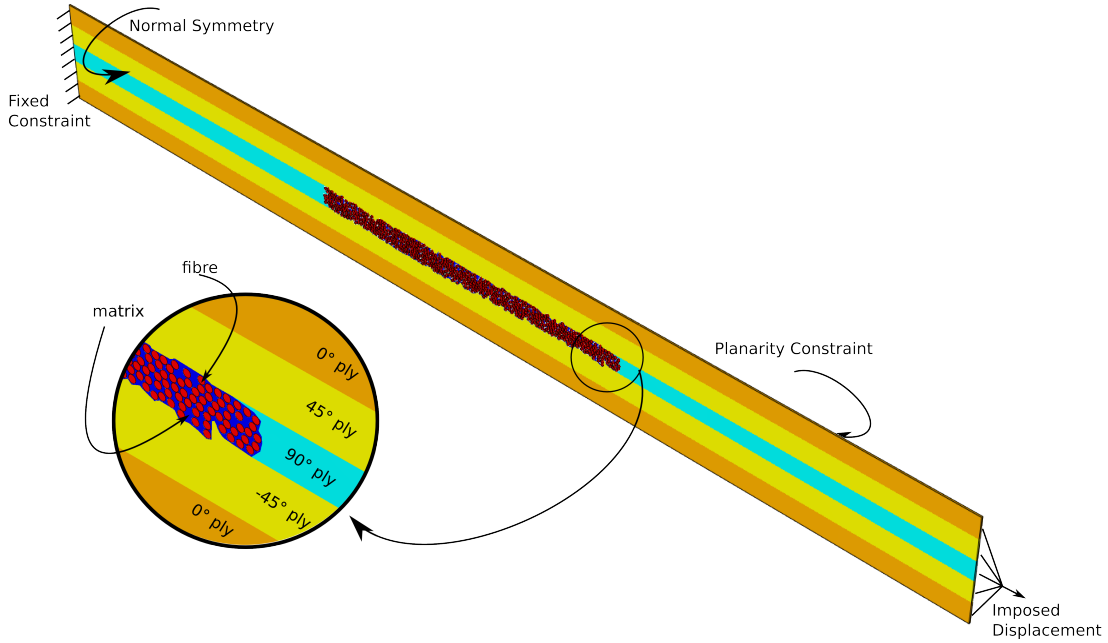

Figure 1. Schematic of the embedded cell plane-strain model of bulk micro damage development

3. Experimental Results

When considering the damage mechanisms at the free edge of the tested samples, a change is observed with decreasing ply thicknesses. In the case of the thickest plies (t = 300 μm), the first cracks appear relatively early with an applied strain comprised between 0.30 and 0.32% and induce an interlaminar delamination process (from 0.5% strain onwards) that carries on until the failure of the specimen (around 0.8% strain). The transverse cracks are shown with red circles at 0.31% strain on such a specimen in figure 2a and the consequent delamination with a blue circle at 0.55% strain in figure 2b. For the t = 150 μm specimens, the onset of matrix cracking is found between 0.41 and 0.51% strain, and shown in figure 2c at 0.5% strain, with the transverse cracking once again highlighted by the red circles. Some matrix cracking induced delamination follows shortly after (0.8% strain) albeit limited in length, which is shown by the blue circle at 0.85% strain in figure 2d. At failure, a higher density of transverse cracks is observed with 0.83 crack/mm in 150 μm plies vs 0.78 crack/mm in 300 μm ones, which is found in agreement with the observations of Sebaey et al. [5]. In the thin-ply specimens with t = 75 μm, shown for instance at 0.9% strain in figure 2e, the onset of matrix cracking is found once again at a higher strain (between 0.52 and 0.66%) than thicker plies. However, the crack density is this time lower than in the 150 μm specimens, which this time shows an opposite trend to the observations of Sebaey et al [5]. It is worth mentioning that plies as thin as this were never studied by these authors, and thus no direct comparisons can be made. In the case of very thin plies (t = 30 μm), neither visible matrix cracking nor delamination can be observed before final failure using optical microscopy at the free edge, as shown in

Excerpt from ISBN 978-3-00-053387-7

figure 2f at 1.05% strain. A typical example for three thicknesses can be found in the inserts of figure 3, with the graph presenting the scaling in total crack density and crack length visually observed at the ultimate tensile strain.

To increase the resolution of the observations, selected specimens were observed in SEM after failure. While transverse cracks are still clearly visible after unloading in SEM for thick ply laminates, no signs of such defects are seen for thin-ply laminates as shown in figure 4, which validates the observations made in-situ with the optical microscope.

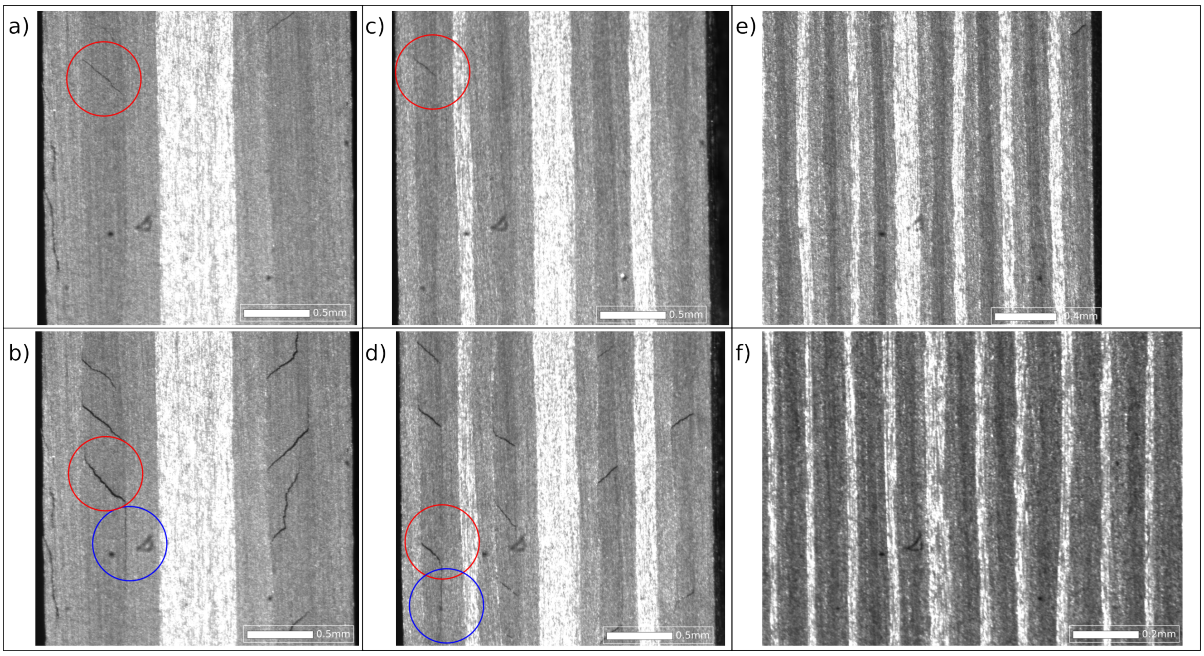

Figure 2. Optical in-situ photographs showing the damage development at the free edge of chosen specimens. Transverse cracking is highlighted in red and matrix cracking induced delamination in blue. (see text for details)

The acoustic emission measurements performed on the test specimens are compared with the ones obtained in Amacher et al. [1] in figure 5, demonstrating the consistency of the experimental procedure and fabrication methods. The ultimate tensile strength is typically within one standard deviation of the previously measured value, whereas the larger difference observed in the acoustic emission measurements for the thicker plies is explained by the difference in loading speed between the two sets of experiments, which could allow for the development of potential viscoplastic behaviour.

Excerpt from ISBN 978-3-00-053387-7

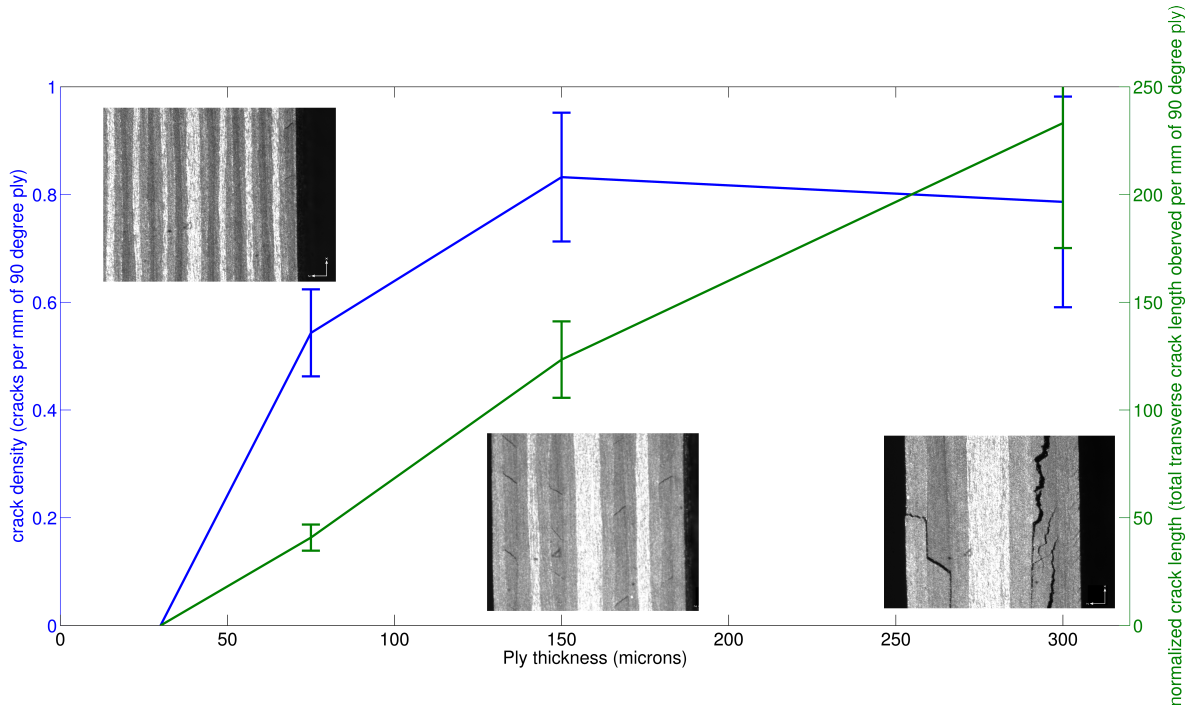

Figure 3. observed crack density and normalized crack length vs ply thickness just before failure

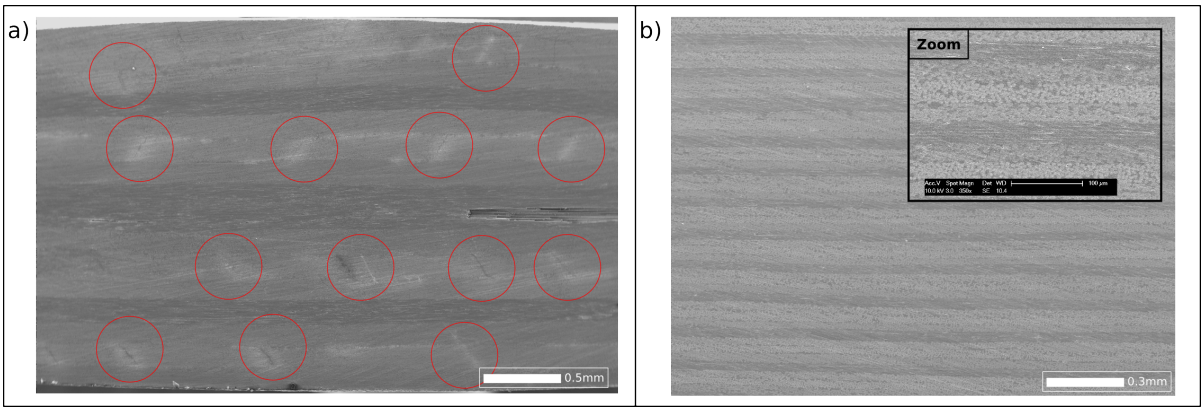

Figure 4. SEM observation of the free edge of a 150 μm sample in (a) with transverse cracks highlighted in red, and a 30 μm sample in (b) with no cracks visible

When comparing the in-situ damage observation at the free-edge with acoustic emission monitoring as is done in figure 5, it is interesting to observe that the first crack visible at the edge of the specimens does not scale in a similar fashion as the onset of damage measured using acoustic emission. For thicker plies, both onsets coincide, meaning that the acoustic emission is able to capture the onset on transverse cracking in standard "thick" ply composites. However, for intermediate ply thicknesses (t = 75 & t = 150 μm), the onset of transverse cracking at the free edge is observed well before the onset of damage determined by acoustic emission (threshold on cumulated acoustic energy). It appears that the limited cracking at the free edge is not sufficient to be detected as a clear onset in the acoustic emission energy profile. However, the acoustic emission energy shows a sudden increase at a value corresponding to the

Excerpt from ISBN 978-3-00-053387-7

measured onset of damage which does not correlate with events recorded at the free edge. Thus, it can be considered that the onset of damage detected by acoustic emission monitoring is representative of a second damage mechanism appearing in the bulk of the laminate and not necessarily at the free edge.

A comparison of the experimentally determined onset of damage with predictions based on the in-situ strength model of Camanho et al. [6] shows a similar trend towards increasing values for thinner plies but fails to quantitatively predict the measured value in its present form as seen in figure 5 where the mode I fracture toughness, G_{Ic}, should be scaled by a factor of 7 to reach perfect agreement for $t = 150\ \mu m$ compared to what had been measured experimentally. The in-situ strength model being based on plain strain assumptions, it is in principle only able to capture effects in the bulk of the specimens, which might explain the observed discrepancy.

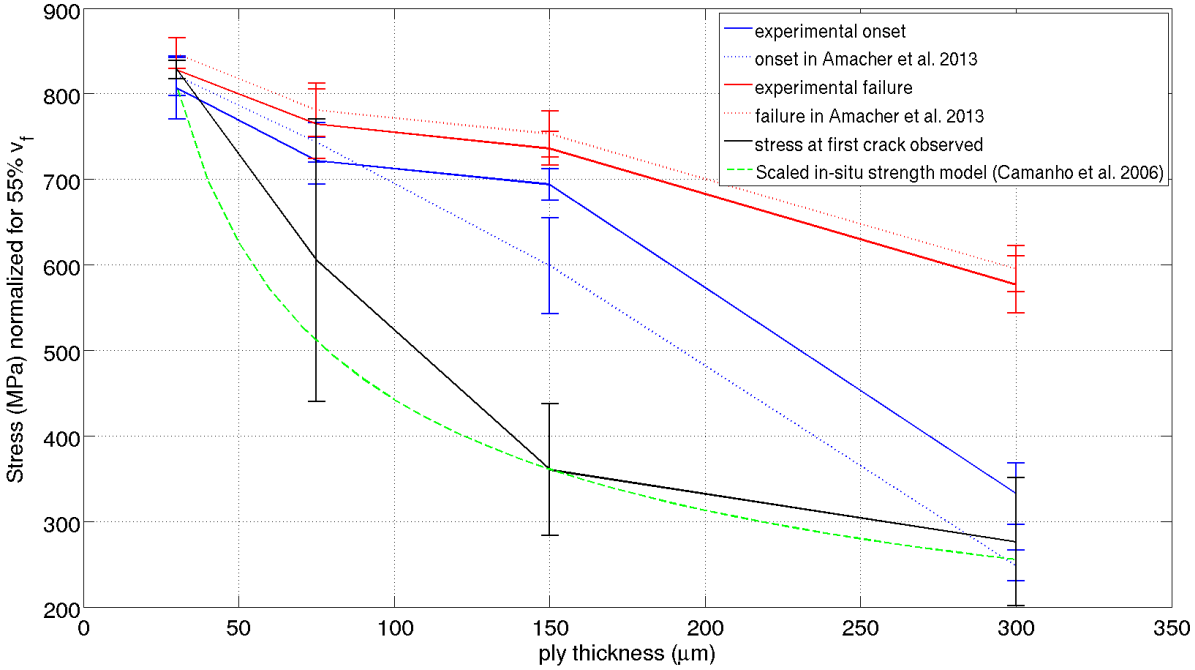

Figure 5. Onset of Damage / First crack observed scaling in tensile tests on quasi-isotropic laminates (M40JB/TP80EP)

4. Numerical modelling

Comparing the strain at onset of transverse cracking in plane strain simulations with the onset measured by acoustic emission in figure 6, a good qualitative agreement was found. A sensitivity study of the model parameters has been performed, which highlighted the major importance of the interface toughness on the results. This value consequently needs to be determined experimentally, but can be expected to fall between the two bounds tested, namely 5 and 10 J/m^2. The typical damage sequence observed is a fibre-matrix debonding in a fibre rich zone, followed by the development of some local plasticity, and ending in matrix damage that propagated through the ply.

Micro-mechanical characterization is also in progress to improve the parameters of the Drucker-Prager model for the matrix by using nano-indentation and the procedure outlined in Rodríguez et al. [7]. DIC measurements during SEM in-situ tensile tests will also be performed to yield important data regarding

Excerpt from ISBN 978-3-00-053387-7

the in-situ behaviour of the matrix and the interface properties. The use of such independent in-situ data will allow a better quantitative agreement to be reached between model and experiments than is currently exhibited.

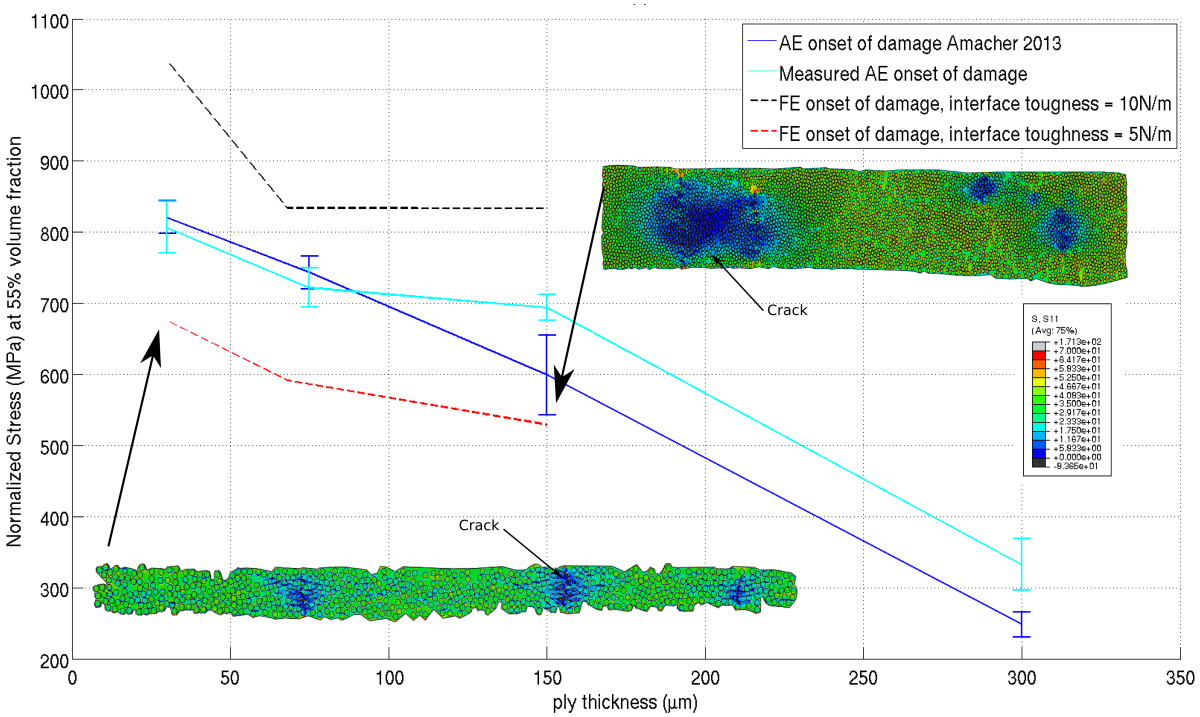

Figure 6. Comparison between AE measurements and FE results

5. Conclusion

The absence of matrix damage for the thinnest plies in the observations made at the free edge, both in-situ and in later SEM investigations, tends to confirm the hypothesis of the existence of a ply thickness limit below which the matrix dominated failure mechanisms are delayed so far that the fibre failure process dominates the failure of the composite [1]. It is also interesting to note that the scaling obtained by acoustic emission measurements and visual observations at the free edge are not similar. The reason why transverse cracking is observed well before reaching the onset of damage determined by the energetic threshold in acoustic emission for intermediate ply thicknesses remains to be investigated, but it can be expected that two separate sets of mechanisms are concurrently at play when performing these unnotched tensile tests. The first set of mechanisms takes place in the bulk of the material in plane strain conditions, and their evolution can be monitored by acoustic emission. The second set takes place at the free edge, and can be monitored using optical or SEM observation of the polished free edge during testing. Consequently, while further work on the plane-strain FE model should yield a better agreement with the experimental result, it can be expected that a full 3D model is required to capture the damage evolution at the free edge. From the tests performed in this study, it is expected that the damage occurring at the free edge dominate the damage evolution of the whole sample for thick ply composites, whereas the response of samples made of thinner plies is dominated by the damage taking place in the bulk of the material, with the free edge damage being constrained there and not propagating inside the sample.

Excerpt from ISBN 978-3-00-053387-7

Acknowledgments

This research was funded by the Swiss National Science Foundation, project 200021_156207

Références

[1] R. Amacher, J. Cugnoni, J. Botsis, L. Sorensen, W. Smith, and C. Dransfeld. Thin ply composites : Experimental characterization and modeling of size-effects. *Composites Science and Technology*, 101 :121–132, 2014.

[2] R. Amacher, J. Cugnoni, J. Brunner, E. Krammer, C. Dransfeld, W. Smith, K. Scobbie, L. Sorensen, and J. Botsis. Towards aerospace grade thin-ply composites. In *ECCM 17*, number aid951_c11448893625, 2016.

[3] Test method for tensile properties of polymer matrix composite materials, 2008.

[4] L.P. Canal, C. Gonzalez, J. Segurado, and J. LLorca. Intraply fracture of fiber-reinforced composites : Microscopic mechanisms and modeling. *Composites Science and Technology*, 72(11) :1223–1232, 2012.

[5] T.A. Sebaey, J. Costa, P. Maimí, Y. Batista, N. Blanco, and J.A. Mayugo. Measurement of the in situ transverse tensile strength of composite plies by means of the real time monitoring of microcracking. *Composites Part B : Engineering*, 65 :40–46, 2014.

[6] P.P. Camanho, C.G. Dávila, S.T. Pinho, L. Iannucci, and P. Robinson. Prediction of in situ strengths and matrix cracking in composites under transverse tension and in-plane shear. *Composites Part A : Applied Science and Manufacturing*, 37(2) :165–176, 2006.

[7] M. Rodríguez, J.M. Molina-Aldareguía, C. González, and J. LLorca. Determination of the mechanical properties of amorphous materials through instrumented nanoindentation. *Acta Materialia*, 60(9) :3953–3964, May 2012.

Excerpt from ISBN 978-3-00-053387-7